

Lawrence Berkeley National Laboratory

Lawrence Berkeley National Laboratory

Title

Recent studies of proton drip-line nuclei using the Berkeley gas-filled separator

Permalink

<https://escholarship.org/uc/item/81r53821>

Authors

Rowe, M.W.
Batchelder, J.C.
Ninov, V.
[et al.](#)

Publication Date

1999-10-07

Recent Studies of Proton Drip-Line Nuclei Using the Berkeley Gas-Filled Separator

M. W. Rowe¹, J. C. Batchelder², V. Ninov¹, K. E. Gregorich¹, K. S. Toth³,
C. R. Bingham^{3,4}, A. Piechaczek⁵, X. J. Xu^{1,6}, J. Powell¹, R. Joosten¹ and
Joseph Cerny^{1,7}

¹Lawrence Berkeley National Laboratory, MS 88, 1 Cyclotron Rd, Berkeley, California 94720

²UNIRIB, Oak Ridge Associated Universities, Oak Ridge, Tennessee 37831

³Department of Physics, Oak Ridge National Laboratory, Oak Ridge, Tennessee 37831

⁴The University of Tennessee, Knoxville, Tennessee 37996

⁵Louisiana State University, Baton Rouge, Louisiana 70803

⁶Institute of Modern Physics, Lanzhou, 730000, China

⁷Department of Chemistry, University of California, Berkeley, CA 94720

Abstract. The Berkeley Gas-filled Separator provides new research opportunities at Lawrence Berkeley National Laboratory's 88-Inch Cyclotron. The use of this apparatus for the study of proton drip-line nuclides is discussed. Preliminary results of ^{78}Kr bombardments of ^{102}Pd targets at mid-target energies of 360, 375 and 385 MeV are presented. Improvements planned partially as a result of this measurement are also discussed.

INTRODUCTION

The properties of proton drip-line nuclides have long been a focus of study at Lawrence Berkeley National Laboratory's 88-Inch Cyclotron. This work includes the confirmation of the first example of direct proton emission, from an isomer of ^{53}Co , in 1970 [1]. However, until recently Berkeley has lacked the optimal tools for the study of proton emitters in the region above Sn, where all subsequent examples of direct proton decay have been observed [2]. Virtually all of these later studies have relied on some form of mass separation or analysis to identify the nuclides of interest and reduce unwanted background from other species produced simultaneously. In fact, it is the development of high resolution mass analyzers and velocity filters, as well as high-granularity silicon detector arrays, which has fueled the recent explosion in knowledge of proton drip-line isotopes in the region between Sn and Bi.

During the Fall of 1998, commissioning of the Berkeley Gas-filled Separator (BGS) began. Although this apparatus was designed primarily as a tool for research on the heaviest elements, its capabilities also make it well suited for the study of proton drip-line isotopes, particularly in the region near lead. After a discussion of the BGS's design and detector systems, preliminary results of the first measurement of very proton-rich nuclides using the BGS will be presented. The primary goal of this experiment was to observe proton emission from ^{177}Tl [3] and ^{176}Tl . In the context of

the results of this measurement, improvements to the BGS which are planned or have already been implemented, will be discussed.

THE BERKELEY GAS-FILLED SEPARATOR

In order to successfully study proton drip-line nuclei, the experimental apparatus used must meet three requirements. Because such isotopes are produced in low yield, the target must be capable of withstanding large beam currents and/or the transport of the products from the target to the detector system must be very efficient. Second, this transport must be accomplished rapidly, since the half-lives of proton emitters are typically on the order of a few tens of milliseconds or shorter [2]. Finally, there must be some way of identifying the proton-emitter in order to distinguish it from other nuclides produced in much higher yields.

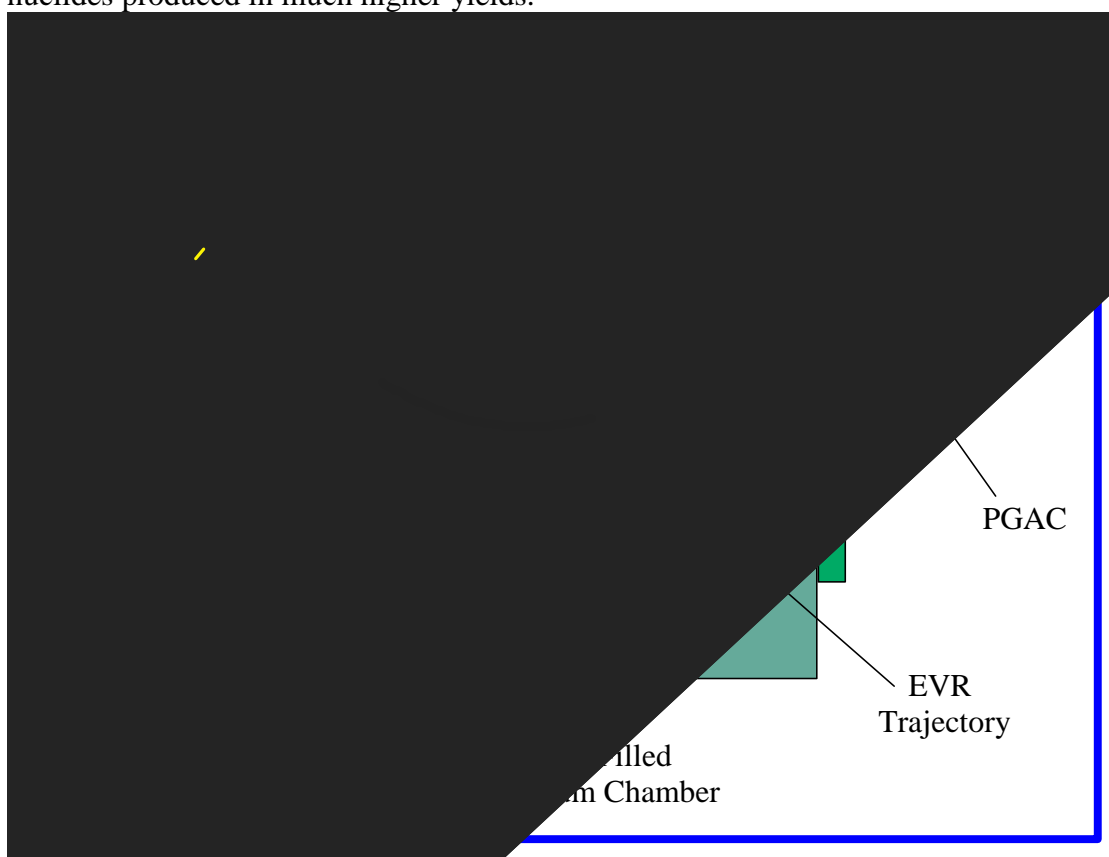


FIGURE 1. A schematic diagram of the Berkeley Gas-filled Separator. The beam enters the apparatus from the left. The detector systems are shown as arranged during the $^{78}\text{Kr} + ^{102}\text{Pd}$ measurement described herein. Recent modifications of the system will be described later in this paper.

Gas-filled separators can fulfill these requirements. The residues of fusion-evaporation reactions emerge from the target in a variety of charge states. Since the magnetic rigidity, upon which the separation of the various products is based, varies as the inverse of the charge, this can substantially reduce the percentage of a given

nuclide transported through the separator to the detector system. To reduce this problem, the magnet of a gas-filled separator is filled with a dilute inert gas. According to Bohr's approximation, collisions with the atoms in the gas will leave the reaction products in an average charge state that is proportional to the cube root of their atomic number. To first order, the resulting magnetic rigidity is proportional to the mass over the cube root of the atomic number. This significantly improves the transport efficiency of a gas-filled separator relative to conventional mass analyzers and velocity filters. Unfortunately, the collisions in the gas cause much of the kinematic information to be lost such that the resolution is only sufficient to separate fusion-evaporation residues from incident beam and direct-reaction products. In effect, the gas-filled separator acts as a purifying beam dump. One must rely entirely on the detector system for identification of the implanted nuclides.

A schematic diagram of the Berkeley Gas-filled Separator is shown in Fig. 1. The beam enters from the left through a $100 \mu\text{g}/\text{cm}^2$ carbon window. The entire apparatus downstream of this window is filled with He gas at a pressure of ~ 1.3 Torr. The gas helps to cool the target, which may either consist of a single foil on a target ladder, or a series of foils mounted on a continuously rotating target wheel. Two PIN-diode detectors behind the target monitor beam elastically scattered from the target. Beam and reaction products exit the target and enter a quadrupole magnet followed by a gradient-field dipole magnet that provide vertical and horizontal focussing, respectively. The latter magnet also increases the separation between beam and fusion-evaporation residues, as does the flat-field dipole that follows. The incident beam is bent such that it is dumped between the two dipole magnets. The focal plane of the system is located inside the detector chamber, approximately 1 m from the exit of the second dipole. The operating parameters of the BGS are presented in Table 1. Note that many of these numbers will depend on the kinematics of the specific reaction employed.

TABLE 1. Operating Parameters of the Berkeley Gas-filled Separator.

Parameter	Value
Maximum beam current:	5×10^{12} ions/s
Target thickness:	0.1 – 1.0 mg/cm ² optimum
Angular acceptance:	± 75 mrad horizontal ± 150 mrad vertical
Momentum acceptance:	$> 50\%$
Charge acceptance:	$\sim 100\%$
Transport efficiency:	20 – 70% typical
Total Bend:	70°
Path Length:	4.6 m
Transport time:	$< 2 \mu\text{s}$
Maximum rigidity:	2.5 T m
Overall background rejection:	$> 10^{12}$
Dispersion:	18 mm / %B ρ
Focal plane image size:	50 mm vertical 80 – 150 mm horizontal

Inside the detector chamber reaction, products pass through a parallel-grid avalanche counter (PGAC) and are subsequently implanted into a $300 \mu\text{m}$ -thick single-sided

silicon strip detector (SSD) located at the focal plane. The SSD is 80 mm wide by 35 mm high. It is divided into 16 vertical strips which give crude position sensitivity in the horizontal plane. Signals are measured from both ends of each strip. The sum of these signals is proportional to the implantation or decay energy. Typical resolution for alpha-decay events was 70 keV full-width at half maximum (FWHM). The ratio of either signal to the sum is used to determine the vertical position of an event along the strip due to resistive charge division. One may think of a particular event occurring within a pixel, defined by the strip and the vertical-position resolution of 900 μm FWHM. The total number of pixels for the focal plane detector is ~ 620 .

Positive identification of a particular reaction product may be accomplished by observing its decay chain if the decays of the daughter nuclides are known. A high-energy signal in the SSD, observed in coincidence with a signal from the PGAC, indicates that a fusion-evaporation residue has been implanted in the silicon detector. One may then look for decays occurring within the same pixel. By time-stamping each event, it is trivial to determine the half-life for a particular decay. Since the residues are implanted near the surface of the detector, the detection efficiency for subsequent decays is approximately 50%. Due to the large number of pixels, the average time between implantations in a given pixel is on the order of seconds, thus permitting the decay chain to be observed through several generations. The decay-correlation technique is particularly well suited for work near the proton drip line where the half-lives of the nuclides of interest are typically less than 50 ms, making false coincidences unlikely. Unfortunately, this technique is not well suited for the region of the proton drip-line immediately below the $N=82$ closed shell, since these nuclides decay primarily by electron capture rather than alpha emission.

A SEARCH FOR LIGHT THALLIUM ISOTOPES

In a first experiment to search for new proton emitters using the BGS, three ^{78}Kr bombardments of a 1.5 mg/cm^2 70%-enriched ^{102}Pd target were performed at mid-target energies of 360, 375 and 385 MeV. Analysis of the data from this experiment is still in progress, and all results presented herein should be considered preliminary. This paper will focus on the results of the 375 MeV bombardment. The goal of this measurement was to reproduce the results of the earlier study of ^{177}Tl performed at Argonne National Laboratory, both to provide energy calibration points and to determine if the BGS was working as expected. Poli, *et al.*[3], produced ^{177}Tl in its ground state using the $^{102}\text{Pd}(^{78}\text{Kr},p2n)$ reaction at 370 MeV with a cross section of 10 nb; an isomer was also produced with a 30 nb cross section. The ground state [$T_{1/2} = 67(37)$ ms] decayed by emission of either an 1156(20) keV proton [27(13)%] or a 6907(7) keV alpha particle. The isomer decayed by emission of a 1958(10) keV proton [51(8)%] or a 7487(13) keV alpha particle with a half life of 451(106) μs .

Figure 2 shows the alpha spectrum measured at the focal plane of BGS during a 17 hour 375 MeV bombardment at an average beam current of approximately 10 pA. Decay events were differentiated from implantations by requiring that they be anti-coincident with signals from the PGAC; no other conditions were applied to generate

this spectrum. The energy resolution for alpha decays was 70 keV. The peaks have been assigned to various Hg, Au and Pt isotopes on the basis of their energies.

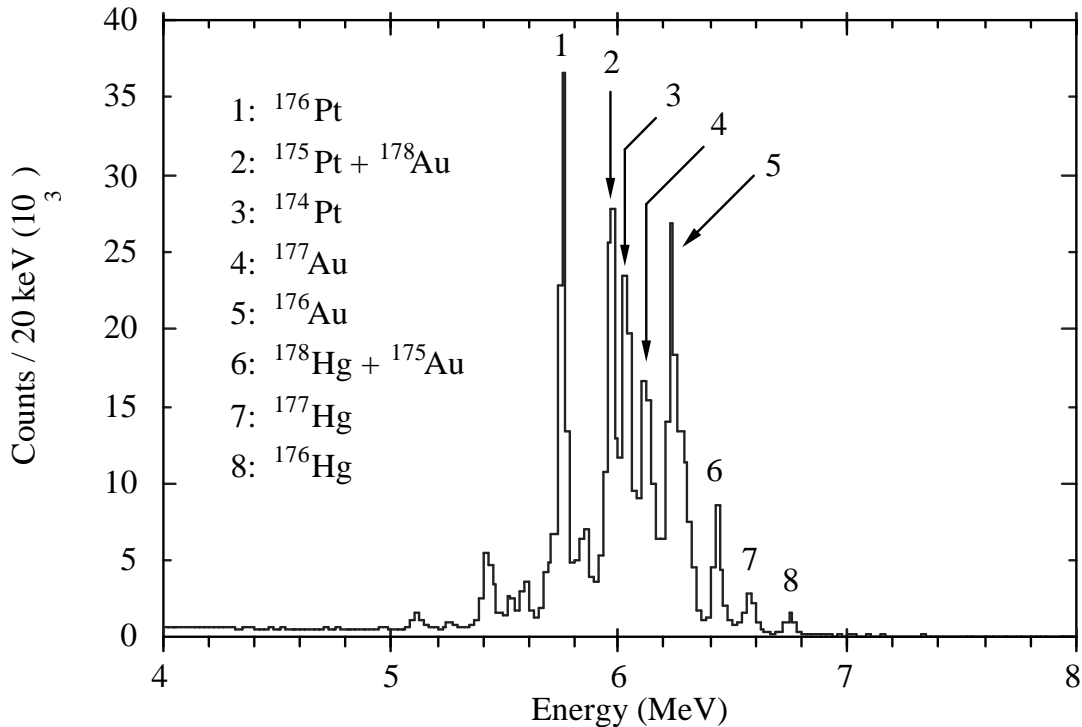


FIGURE 2. Alpha decays observed during the 375 MeV ^{78}Kr bombardment of ^{102}Pd . All events shown were detected in anti-coincidence with signals from the PGAC. Preliminary assignments have been made for some of the peaks based on their energies.

When compared to the work of Poli and collaborators [3], one sees that the distribution of isotopes produced was slightly different. This may be due in part to the somewhat higher beam energy employed. Based on the yield of two key isotopes, ^{177}Hg and ^{177}Au , it would appear that the transport efficiency of the BGS was significantly lower than had been expected. Several factors may have contributed. In an effort to increase the suppression of the primary beam at the focal plane, a stack of carbon degrader foils, with a total thickness that was varied from 1.09 to 0.76 mg/cm^2 , was placed immediately behind the target. This may have adversely affected the BGS optics and lowered transmission. Subsequent measurements suggest that these foils were not necessary to achieve adequate beam suppression. These foils also blocked the elastic scattering detectors used to measure beam current, so it is unclear how accurate the beam intensity cited above is. Finally, much of the time was spent attempting to optimize the tune of the separator. At the time of this measurement, the analysis code was still in development, which complicated tuning due to lack of on-line diagnostics. However, the yield of alpha emitters was within a factor of two of that measured using the Fragment Mass Analyzer at Argonne [3], and this result was achieved in a shorter time period (17 hours vs. 65 hours).

In order to positively identify the various isotopes produced, correlations were sought between the implantation of evaporation residues and the subsequent chain of decays. A time stamp for each event was generated using independent MHz, kHz and Hz clocks. During analysis, all events coincident with signals in the PGAC were assumed to be implantations and stored in a correlation buffer. When a decay event was observed, a search was made for earlier implants or decays within 0.9 mm on the same strip of the SSD. The maximum preceding time interval that was searched for correlations was determined by the energy of the event in accordance with typical half-lives; for alpha decays of greater than 6.7 MeV, this was set to 150 ms. When correlations were found between alpha decays and earlier events, the decays were added to the correlation buffer as well.

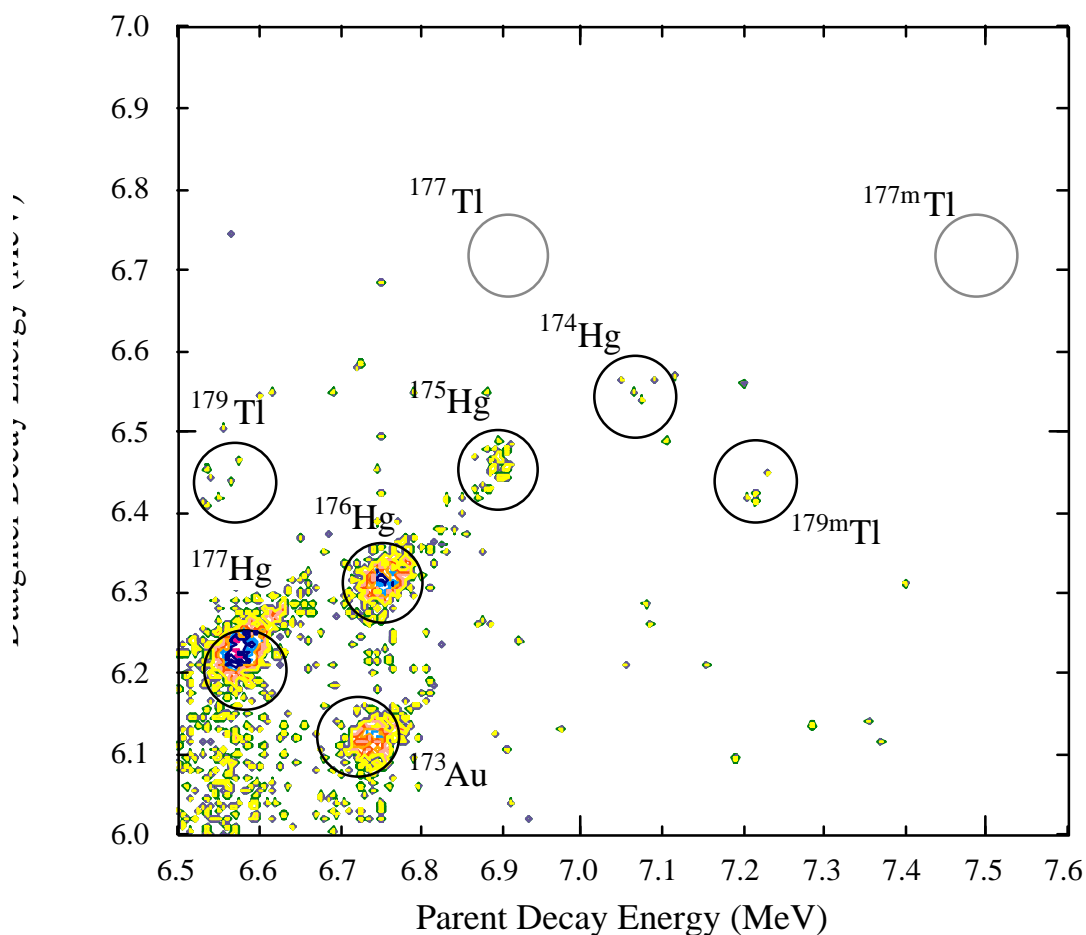


FIGURE 3. A parent-daughter alpha-decay correlation plot generated from the data collected during the 375 MeV ^{78}Kr bombardment. See text. The contour lines increase logarithmically; black indicates the 8-count contour.

Figure 3 shows a correlation plot between successive generations of alpha decays from the same data set that generated Fig. 2. The decay energy from the parent lies along the x-axis and the subsequent decay is plotted on the y-axis. The circles, which

have a diameter encompassing 100 keV, indicate the positions of various parent-daughter decay series, as based on their literature decay energies [4]. Each is labelled with the parent isotope. The ^{177}Hg - ^{173}Pt , ^{173}Au - ^{16}Ir , ^{176}Hg - ^{172}Pt and ^{175}Hg - ^{171}Pt parent-daughter decay pairs are clearly seen. Several events are observed which correspond to the decay energies for the ground state and isomer of ^{179}Tl and their daughter ^{175}Au . No evidence is observed of the decays of ^{177}Tl or $^{177\text{m}}\text{Tl}$ as indicated in the grey circles. However, several correlated events are observed which have the same decay energies as ^{174}Hg and ^{170}Pt . Though additional analysis will be required to confirm this assignment, this is very encouraging, since only a few ^{174}Hg decay events have been observed in previously published studies [5, 6].

A search was also made for protons correlated with alpha decays. For these purposes, all events with energies between 1 and 2 MeV that were anti-coincident with signals from the PGAC were considered to be protons. Since proton emission from high-spin isomers can occur with a relatively long half-life, a maximum correlation-search time of 500 ms was used. A position resolution of 0.9 mm was also used again as the condition for spatial correlation. Using these criteria, only six event pairs were found in the 375 MeV data set with a proton correlated to an alpha decay with an energy greater than 6.5 MeV.

Table 2 shows the data for two of these events which are ^{177}Tl candidates. The first three columns from the left show the type of event observed, followed by the time interval and difference in position between an event and the correlated event which preceded it. The next three columns show the nuclide to which the decay is tentatively assigned, and the decay energies and half-lives, taken from the literature [4]. The first event is assigned to the decay chain of the ^{177}Tl isomer. There is excellent agreement between the energies observed and previously measured values of the $^{177\text{m}}\text{Tl}$ decay chain, and all four events (including the implantation) occur very close together on a single silicon strip. However, the time intervals between the implantation and the first two decays are much longer than would be expected from the literature half-lives. It should be noted that the scalars used to generate the time stamps for each event would occasionally give bad values. A great deal of effort was required to correct for this problem in the analysis, and thus the timing information is somewhat suspect. However, there is virtually no doubt that all of these four events occurred within a very short time period. The second candidate is assigned to the ^{177}Tl ground-state decay. Again, there is excellent agreement between decay energies, and the events occur very near to one another. Also, the decay times are in better agreement with the half-lives for this chain, though the above stipulations still apply.

TABLE 2. Candidate ^{177}Tl Events Compared to Literature Values.

Decay Chain	Δt	Δy	Nuclide	Literature Decay	Half-Life
(EVR implanted)					
1930 keV proton	53 ms	+0.21 mm	$^{177\text{m}}\text{Tl}$	1958 keV proton	451 μs
6760 keV alpha	358 ms	-0.23 mm	^{176}Hg	6740 keV alpha	30 ms
6310 keV alpha	73 ms	-0.29 mm	^{172}Pt	6310 keV alpha	100 ms
(EVR implanted)					
1110 keV proton	1.5 ms	+0.09 mm	$^{177\text{g}}\text{Tl}$	1156 keV proton	67 ms
6710 keV alpha	22 ms	-0.14 mm	^{176}Hg	6740 keV alpha	30 ms

OUTLOOK FOR THE FUTURE

These preliminary results are quite encouraging. However, this experiment also made it clear that the BGS, in its original configuration, had several shortcomings. In the months since, a variety of improvements have been planned and, in most cases, implemented. Figure 4 is provided to illustrate some of the problems with the original configuration of the separator and its detectors. It shows energy spectra measured in the SSD at the focal plane during the 360 MeV ^{78}Kr bombardment. The black line shows the sum of all events measured at the focal plane. The dark grey line shows the subset of those events which were coincident with signals from the PGAC, and thus interpreted as implantations of fusion-evaporation residues. The light grey line shows events that were anticoincident with PGAC signals, and therefore interpreted as decays.

It is seen that the majority of events above 2 MeV in Fig. 4 are coincident with the PGAC. However, between 5 and 7 MeV alpha decay signals dominate. Above, 7 MeV, virtually no alpha decays should be observed, so it is clear that some implantation events are passing through the PGAC without producing a signal. To improve the discrimination between implant- and decay-type events, a second PGAC was added to the BGS upstream of the focal plane shortly after this experiment. This greatly improves the discrimination.

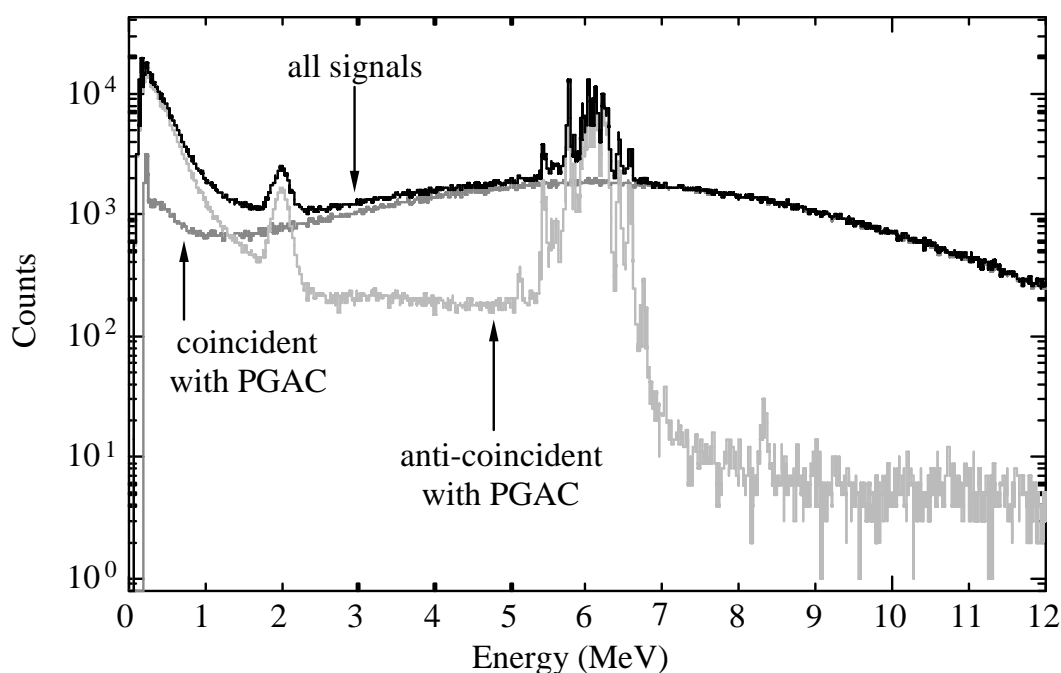


FIGURE 4. Energy spectra of events observed in the silicon strip detector (SSD) located at the BGS focal plane. The black line indicates the spectrum of all events. The heavy and light grey lines indicate the subsets of those events which were either coincident or anticoincident with PGAC signals, respectively.

A broad peak which is mostly anticoincident with the PGAC is seen in the spectrum near 2 MeV. This is due to high-energy He ions resulting from collisions between heavy ions and the He gas in the BGS. Because they are high-energy and low-Z, they produce minimal signals in the PGAC and are not stopped in the SSD. Soon after this experiment, a second silicon strip detector was put in place behind the focal plane SSD. Events observed in coincidence with signals > 1 MeV from this detector are discarded. The small peak near 8 MeV is of unknown origin, but may have been caused by a similar mechanism. It does not seem to be correlated with alpha decay chains.

As noted earlier, the energy and position resolution of the SSD average approximately 70 keV and 0.9 mm, with some strips behaving much worse than others. This was due to radiation damage sustained during the commissioning of the BGS. This was later improved somewhat by annealing the detector. It is planned that this SSD will be replaced early in 2000 by two 60 mm x 60 mm 16-strip silicon detectors placed side-by-side at the focal plane. Besides improving the energy and position resolution, this will also provide more focal plane coverage. The enhanced position sensitivity will increase the average time between implantations at a given position by a factor of approximately 8, decreasing the chances of false coincidences between different decay chains. This should permit more decay generations to be observed, or higher event rates to be tolerated.

Most of the decay events observed below 5 MeV in Fig. 4 are due to alpha particles which decay out of the detector, so that only a partial energy signal is observed. To improve this situation, six additional SSD's will be placed around the four sides of the focal plane SSD, perpendicular to its surface. These will detect approximately 60% of the alpha particles or protons that escape from the focal plane detector. In addition to increasing the odds of observing decay chains through multiple generations, this will reduce the "background" in the region between 1 and 2 MeV where proton decays will be observed. These side detectors will also be installed in early 2000.

During this experiment, the dead time of the data acquisition system after each event was about 200 μ s. This would prevent the observation of isotopes with very short half-lives. The CAMAC-based system which was used is being replaced by a VME-based system, which should significantly reduce this problem. This is especially important due to the large number of additional channels which will be needed for the new detectors described above. There have also been improvements in the data analysis code that will improve on-line diagnostics.

Finally, experience with tuning the separator will also prove important. In particular, recent measurements have indicated that suppression of the primary beam is sufficient in this reaction without degrading the beam and recoils after the target. In Fig. 4, the evaporation residues have been degraded to the same energy range as the alpha decays. Without the carbon degrader foils, the occasional implant event that does not produce a signal in the PGAC is unlikely to be mistaken for a decay. Also, the elastic scattering detectors behind the target will no longer be blocked by degrader foils, so the beam intensity may be accurately assessed.

If necessary, we plan to repeat this experiment in order to take advantage of these improvements to the BGS. In addition, several other measurements of proton and alpha-particle emitters in this region of the Chart of the Nuclides are planned. These

studies will provide important decay, mass and structure information about nuclei at the extreme limits of stability.

CONCLUSION

Although yields observed in this early BGS experiment were not as high as had been expected, the results of the preliminary analysis of the 375 MeV data are intriguing. Much more work still remains to be done on the analysis at this time; only about half of the 375 MeV data has been examined. Improvements in the correlation algorithms may also yield additional results which were missed. Analysis of the data taken at 360 MeV and 385 MeV has only been cursory at this point.

Partially as a result of this experiment, a series of improvements to the BGS are being implemented. Some of these improvements were in place during the element 118 measurements [7], and proved to be critical to the success of those experiments. The present study has indicated that the BGS will be an excellent tool for the investigation of proton drip-line nuclei near the $Z=82$ shell closure. In particular, its high transport efficiency and its ability to utilize high beam intensities will permit isotopes produced in very low yields to be observed and identified. This will be especially true once all of the planned improvements are in place.

ACKNOWLEDGMENTS

We wish to acknowledge the excellent work David Ruiz, Ron Oort and the rest of the 88" Cyclotron machine shop and technical staff did in building and installing the BGS. We also thank Sigurd Hofmann and GSI for the silicon strip detector used in this measurement, and the 88" Cyclotron operations staff for their assistance with this experiment. This work was supported by the U. S. Department of Energy under contracts DE-AC03-76SF00098 (Lawrence Berkeley National Laboratory), DE-AC05-76OR00033 (UNIRIB), DE-AC05-96OR22464 (Oak Ridge National Laboratory, managed by Lockheed Martin Energy Research Corporation), DE-FG02-96ER40983 (University of Tennessee), and DE-FG02-96ER40978 (Louisiana State University).

REFERENCES

1. Cerny, J., Esterl, J. E., Gough, R. A. and Sextro, R. G., Phys. Letters 33B, 284-286 (1970).
2. Woods, P. J., and Davids, C. N., "Nuclei Beyond the Proton Drip-Line," in Ann. Rev. Nucl. Part. Sci., 47, 541-90 (1997).
3. Poli, G. L., *et al.*, Phys. Rev. C 59, R2979-R2983 (1999).
4. Pfennig, G., Klewe-Nebenius, H., Seelmann-Eggebert, W., Karlsruhe Chart of the Nuclides, 6th ed., revised reprint, Institute fuer Instrumentelle Analytik, 1998.
5. Uusitalo, J., *et al.*, Z. Phys. A 358, 375-376 (1997).
6. Seweryniak, D., *et al.*, Phys. Rev. C 60, 031304-1—031304-4 (1999).
7. Ninov, V. *et al.*, Phys. Rev. Lett. 83, 1104-7 (1999).